Mohsenzadeh, A., *et al*.: Convective Cooling of Tandem Heated Triangular Cylinders ...
THERMAL SCIENCE: Year 2010, Vol. 14, No. 1, pp. 183-197

183

CONVECTIVE COOLING OF TANDEM HEATED TRIANGULAR CYLINDERS CONFIRM IN A CHANNEL

by

Afshin MOHSENZADEH, Mousa FARHADI [*]*, and Kurosh SEDIGHI*

Faculty of Mechanical Engineering, Babol Noshirvani University of Technology,
Babol, Islamic Republic of Iran

Numerical simulations of forced convective incompressible flow in a horizontal plane channel with adiabatic walls over two isothermal tandem triangular cylinders of equal size are presented to investigate the effect of wall proximity of obstacles, gap space (i. e. gap between two squares), and Reynolds number. Computations have been carried out for Reynolds numbers of (based on triangle width) 100, 250, and 350 . Results show that, wall proximity has different effect on first and second triangle in fluid characteristics especially in lower gap spaced, while for heat transfer a fairly same behavior was seen.

Key word: *unsteady laminar flow, convective heat transfer, tandem triangles, wall proximity*

Introduction

The flow over bluff bodies occurs in many engineering applications such as the cooling of electronic components, heat exchangers, and aerodynamic fields. One of the basic configuration that can be used as a bluff body is triangular obstacle [1-7]. By reviewing literature, it reveals that it has not been studied enough especially in heat transfer field. Alonso *et al*. [1] analyzed the effect of cross-section shape and angle of attack on galloping stability of two-dimensional triangular cross-section bodies through static wind tunnel experiments. They found that galloping stability depend on both cross-section shape and angle of attack. Buresti *et al*. [2] carried out an experimental investigation for triangular prisms with two different cross-sections (*i. e*. equilateral and isosceles with 90º apex angle). They tried to find critical aspect ratio that below it, vortex shedding shift from alternate type (*i. e*. the usual Karman alternate shedding of vortices from the two sides of the body) to second type of shedding (*i. e*. a symmetrical shedding of "arch-type" vortices). But, just alternate vortex shedding was find for all aspect ratio. Csiba *et al*. [3] investigated experimentally influence of incidence angle on Strouhal number of an isosceles triangle. They showed when Strouhal number defined based on triangle width (B), the Strouhal number increases with incidence angle, α, but when the Strouhal number defined based on $B' = B\cos\alpha$ as a length scale, Strouhal number is independent of α. The laser Doppler

---

* Corresponding author; e-mail: mfarhadi@nit.ac.ir

Mohsenzadeh, A., *et al*.: Convective Cooling of Tandem Heated Triangular Cylinders ...

184   THERMAL SCIENCE: Year 2010, Vol. 14, No. 1, pp. 183-197

velocimetry (LDV) study of Ulrichs *et al*. [4] over a right-angled triangle about the separation behavior of bluff bodies in the vicinity of a wall showed that when triangle is placed in the vicinity of the wall there will be two separation regions: (1) bluff body separation region, and (2) wall bounded separation region. As triangle moves away the wall, the wall bounded separation region eventually disappears. Abbassi *et al*. [6] carried out a numerical investigation to study forced convection of air for a two-dimensional unsteady-laminar flow in a horizontal channel with a built-in triangular prism. They showed that the presence of triangular prism for symmetric flow (Re < 45) has just a little local effect on heat transfer from the channel wall. In contrast at the periodic flow (Re ≥ 45) presence of triangular prism has an important effect in enhancement of heat transfer from the channel wall. Chattopadhyay [7] studied same geometry but for turbulence flow. In this case an augmentation of about 17% in averaged Nusselt number is recorded.

When the bluff body is placed in the channel, depending on the position of obstacle, different flow created, when obstacle is placed in the center of channel, there is a periodic flow with vortex shedding, as obstacle approaches the wall, flow becomes asymmetric and for sufficient wall approach ratio (*a/h*) flow becomes suppressed and there is not vortex shedding any more, this critical wall approach ratio depend on the boundary layer thickness (δ/D) and Reynolds number. It has been reported different critical wall approach by authors at high Reynolds numbers. Martinetuzzi *et al*. [8] and Bailey *et al*. [9] reported critical gaps width of S/D = 0.3-0.4 at Re = 18900 and δ/D = 0.5. While Bosch *et al*. [10] suggest critical gaps width of S/D = 0.13 at Re = 22000, δ/D = 0.13. Chakrabarty *et al*. [11] carried out an experimental investigation into the effect of wall proximity on heat transfer and flow field around a rectangular prism for the Reynolds number 4.9·10⁴, different blockage ratios, aspect ratios, height ratios, and various angles of attack. They observe that the drag coefficient (C_d) and local Nusselt number (Nu) for all blockage ratios and angles of attack decrease as the prism approaches the upper wall. Singha *et al*. [12] carried out an numerical investigation into the effect of wall proximity on heat transfer and flow field around a circular cylinder for the Reynolds number in the range 200-250 and wall approach ratio (ratio of distance of the cylinder from the wall to the diameter of the cylinder) between 0.1-2.5. They found that as cylinder approaches the wall, vortex shedding regime from two rows of vortices of opposite-sign changes to single row vortices of same-sign. Flow also becomes suppressed under the critical wall approach ratio.

On the other hand the unsteady, viscous flow past two bluff bodies such as square [13-17] and circular [18-22] cylinders has been the focus of numerous numerical and experimental investigations. Rosales *et al*. [13] studied numerically a tandem pair of squares of unequal sides (*i. e*. eddy square that is adiabatic and heated square) in channel flow at Re = 500 and gap space equals 2 based on side length of the heated cylinder. They investigated the effect of wall proximity of obstacle on heat transfer from heated obstacle and flow field in inline and stagger position. They showed in inline position where the heated square is placed in the center of channel, there is not any vortex shedding in the gap space between two obstacle unlike stagger arrangement that vortex sheds on the gap space. On the other hand when the obstacles approach the wall in inline arrangement, vortexes start to shed in the gap space. They showed that the drag coefficient, Strouhal number, and Nusselt number of the cylinder decrease as the heated cylinder approach the wall. Valencia [14] studied flow field and heat transfer characteristics in a plane channel with two rectangular cylinder placed perpendicular to the flow direction in the channel center plane for 100 ≤ Re ≤ 400, 1 ≤ *S/B* ≤ 4. He found that flow is steady at Re = 100 for all gap space and the heat transfer enhancement on the channel walls is about 78% for *S/B* = 2, 3,

and 4 at Re = 400 while it is only 8% for S/B = 1. Farhadi *et al.* [15] investigated numerically effect of blockage ratio, gap space between obstacle and Reynolds number on forced convective incompressible flow in a horizontal plane channel and heat transfer over two isothermal tandem square cylinders. They showed increasing blockage ratio has a negative effect on heat transfer from second square and for high gap space, as vortex sheds in the gap between square, the drag coefficient and the Nusselt number both increase in the second square in comparison to the first square.

Sumner *et al.* [18] studied vortex shedding for different gap space and incidence angle, they found behavior of Strouhal number depends on whether the cylinders were closely, moderately, or widely spaced. A large body of evidence about group of cylinders in cross-flow given by Zdravkovic [19] and evidence about critical distance, can be found in Kostic *et al.* [20]. Akbari *et al.* [21] studied flow patterns around two staggered circular cylinders in cross-flow at Re = 800. They found five distinct flow regimes, depending on pitch ratio and angle of incidence. Buyruk [22] studied tandem circular cylinder at Re = 400 to investigate the effect of gap space between cylinder on heat transfer. He showed for high gap space, curve trend of heat transfer coefficients are similar while for lower gap space, they changed. He also showed that laminar boundary layer region heat transfer of first cylinder is not affected by decreasing of gap space.

Governing equation

The flow is assumed unsteady, two-dimensional and laminar, for which the governing conservation equations of mass, momentums, and energy can be written in the following forms:

$$\frac{\partial u}{\partial x} + \frac{\partial v}{\partial y} = 0 \tag{1}$$

$$\frac{\partial u}{\partial \tau} + \frac{u \partial u}{\partial x} + \frac{v \partial u}{\partial y} = -\frac{\partial P}{\partial x} + \frac{1}{\text{Re}} \left(\frac{\partial^2 u}{\partial x^2} + \frac{\partial^2 u}{\partial y^2} \right) \tag{2}$$

$$\frac{\partial v}{\partial \tau} + \frac{u \partial v}{\partial x} + \frac{v \partial v}{\partial y} = -\frac{\partial P}{\partial x} + \frac{1}{\text{Re}} \left(\frac{\partial^2 v}{\partial x^2} + \frac{\partial^2 v}{\partial y^2} \right) \tag{3}$$

$$\frac{\partial \theta}{\partial \tau} + \frac{u \partial \theta}{\partial x} + \frac{v \partial \theta}{\partial y} = \frac{1}{\text{Re Pr}} \left(\frac{\partial^2 \theta}{\partial x^2} + \frac{\partial^2 \theta}{\partial y^2} \right) \tag{4}$$

In the above equations u, v, θ, P, Re, and Pr are dimensionless fluid velocities, temperature, pressure, Reynolds number, and Prandtl number (Pr = 0.71), respectively. The dimensionless forms of the variables are:

$$x = \frac{x^*}{B}, \quad y = \frac{y^*}{B}, \quad \tau = \frac{t u_{\text{max.}}}{B}, \quad u = \frac{u^*}{u_{\text{max.}}}, \quad v = \frac{v^*}{u_{\text{max.}}}, \quad P = \frac{P^*}{\rho u_{\text{max.}}^2}, \quad \theta = \frac{T - T_C}{T_H - T_C} \tag{5}$$

The thermal heat flux exchanged between the walls and the flow is specified by the streamwise-averaged Nusselt number calculated as follows:

$$\overline{\mathrm{Nu}} = \frac{1}{\dfrac{L}{B}} \int_0^{L/B} \mathrm{Nu}\, \mathrm{d}l \tag{6}$$

where Nu is the local Nusselt number which is defined as:

$$\mathrm{Nu} = -\frac{\partial \theta}{\partial n} \tag{7}$$

The streamwise- and time-averaged Nusselt number is defined as:

$$\langle \overline{\mathrm{Nu}} \rangle = \frac{1}{t_1} \int_0^{t_1} \overline{Nu}\, \mathrm{d}t \tag{8}$$

where t_1 is the total time.

Computational domain and boundary condition

The computational domain is shown in fig. 1. Geometry considered is a horizontal channel with two tandem isosceles triangles with 90º apex angle, placed at the distance *a* from upper wall. The dimensionless channel length is equal to $L/B > 20$ and the upstream distances, *Lu*, is selected as 4*B*. The triangle bottom width (*B*) was selected as *H*/4 which corresponds to the blockage ratios of 0.25. The distance between two triangle was changeable ($S/B = 1, 2, 3, 4$).
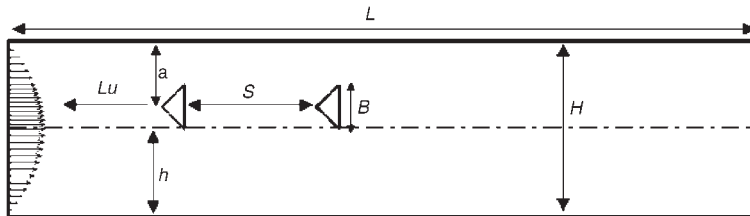

**Figure 1. Geometry
of the problem**

At the channel inlet, the local normal component of velocity is assumed to be zero, and a fully developed parabolic profile for the axial velocity prescribed:

$$u^* = u^*_{\mathrm{max.}} \left[1 - \left(\frac{y}{y_B} \right)^2 \right], \quad v^* = 0 \tag{9}$$

where u^*, v^* are local components of velocity, and $y_B = h$, and the incoming stream is assumed to be at constant temperaturle *TC*, while the triangular obstacles are at a temperature *TH* that $TH > TC$. The bottom and top wall of channel are adiabatic. No-slip boundary conditions for the velocity are imposed on the upper and lower channel walls and the cylinder surfaces. At outlet the convective boundary condition (CBC) is as follow:

$$\frac{\partial \phi}{\partial \tau} + U \frac{\partial \phi}{\partial X} = 0 \tag{10}$$

where ϕ is any of the dependent variables and U is a mean dimensionless velocity on the out-flow.

Numerical procedure and validation

The mentioned equations in pervious section are solved by unsteady turbulent flow at non-orthogonal co-ordinates (UTFN) code which is a computer code for computation of two dimensional steady/unsteady and turbulent/laminar flows in FORTRAN. This code has been generated at 2005 by Nourollahi [23]. The finite volume method is applied to transfer the partial differential equations to algebraic relations. Then the strongly implicit procedure (SIP) algorithm is used to solve the obtained algebraic equations. The present code utilize the collocated variable arrangement and use Cartesian velocity components in which all variables are stored at the same control volume. In order to solve the Navier-Stokes and continuity equations the SIMPLE method supplying the pressure-velocity coupling, is used. This method has its origin in staggered grid methodology and is adapted to collocated grid methodology through the use of Rhio and Chow interpolation [24]. This interpolation can increase the stability of solution too. The unsteady term is discretized by a three time level method. In addition three different discretization schemes are available to approximate the convective terms, upwind/central difference and hybrid schemes. Diffusion term is discretized by central difference scheme (CDS). In this study, the convection and diffusion terms of the equations are discretized by CDS. Further details about the numerical method are given in Nourollahi [23].

A non-uniform grid that is non-orthogonal before the obstacles is used with a minimum spacing near the sides of obstacle and stretching with the fix factor. To check grid independence in this work, one case was run ($S/B = 3$, $a/h = 0.75$) for Re = 350. Table 1 shows the results of grid dependency for time and space-averaged

Table 1. Results of grid dependence

Grid	$\Delta x_{min.}, \Delta y_{min.}$	$\langle \overline{\text{Nu}} \rangle_{first\ obdtacle}$	$\langle \overline{\text{Nu}} \rangle_{second\ obstacle}$
187×68	$0.0231B$	5.1079	3.5460
215×89	$0.014B$	5.3428	3.5886
230×98	$0.0087B$	5.3854	3.5939

Nusselt number. Results show that, when the number of grid points passes from a 187×68 to 215×89, the space and time-average Nusselt number increases 4.6% and 1.2% for first and second triangle, respectively. But when the number of grid points pass from 215×89 to 230×98, it increases only 0.8% and 0.14%. These grid points have minimum grid spacing $0.0231B$, $0.014B$, and $0.0087B$ for 187×68, 215×89, and 230×98, respectively. Therefore the minimum grid spacing $0.014B$ is sufficient and is retained for other investigations.

This case corresponds to the work of Abbasi *et al.* [6]. The instantaneous vectors pattern for Re = 100 was presented and compared with the result of ref. [6] at fig. 2. This figure shows a good agreement of present data in comparison with other numerical result. Table 2 shows the time and streamwise-averaged Nusselt number over the lower wall of the channel. It can be observed a reasonable agreement between the results of this work and the previous studies.
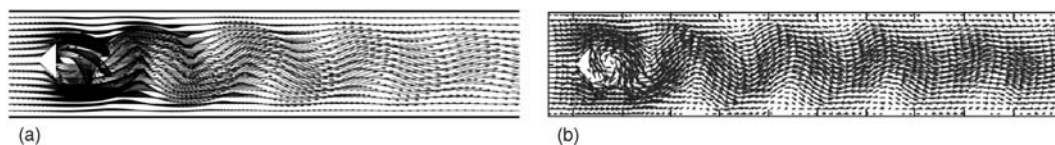

(a)   (b)

Figure 2. The instantaneous vectors plot of (a) present study and (b) Abbasi *et al.* [6]

Mohsenzadeh, A., *et al.*: Convective Cooling of Tandem Heated Triangular Cylinders ...

188   THERMAL SCIENCE: Year 2010, Vol. 14, No. 1, pp. 183-197

Table 2. Comparison $\langle \overline{\mathrm{Nu}} \rangle$ between present work with the previous numerical study [6]

Re	Present study	Abbasi *et al.* [6]
30	0.71	0.68
100	1.58	1.44
150	2.06	1.96
250	2.62	2.51

Results

Flow field

In this part the effect of the Reynolds number, wall approach ratio (*a/h*) and gap between two triangular cylinders (*S/B*) over the flow field and flow characteristic such as the drag coefficient and Strouhal number were investigated. Figure 3 shows the time-averaged streamlines for different wall approach and gap ratios (*S/B*) at Re = 100. It is observed that a small circulation zone is formed along the lower side of the second triangle in the gap between two triangle at *S/B* = 1 and *a/h* = 0.5. This phenomenon can be observed at all Reynolds number – fig. 4(a). It is because of the reverse flow which created by positive pressure gradient over the lower side of the second triangular. This circulation zone is removed by increasing the *S/B* at *a/h* = 0.5 (fig. 3). It is due to changing the flow direction which removes the adverse pressure gradient over the lower side of the cylinder by increasing the *S/B*. Results show that the vortex does not shed between two cylinders at Re = 100 and *a/h* = 1 except *S/B* = 4 which shows a weak shedding in this area. Wall approach ratio has a main effect on the vortex formation between cylinders and downstream of the second triangular cylinder.
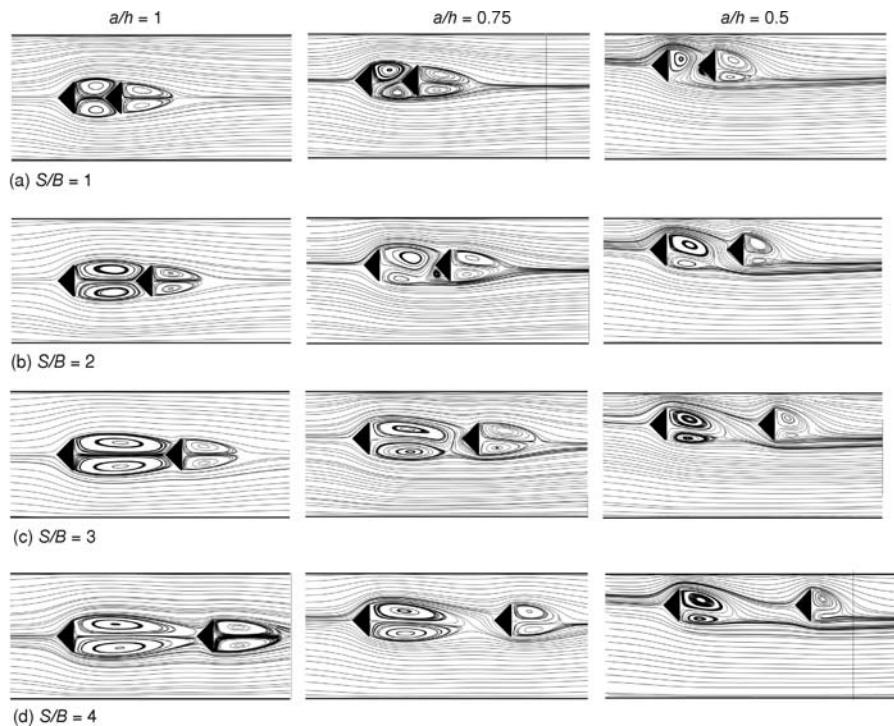

Figure 3. Time-averaged streamlines for wall approach ratio *a/h* = 1 (left), *a/h* = 0.75 (center), and *a/h* = 0.5 (right) at different *S/B* for Re = 100
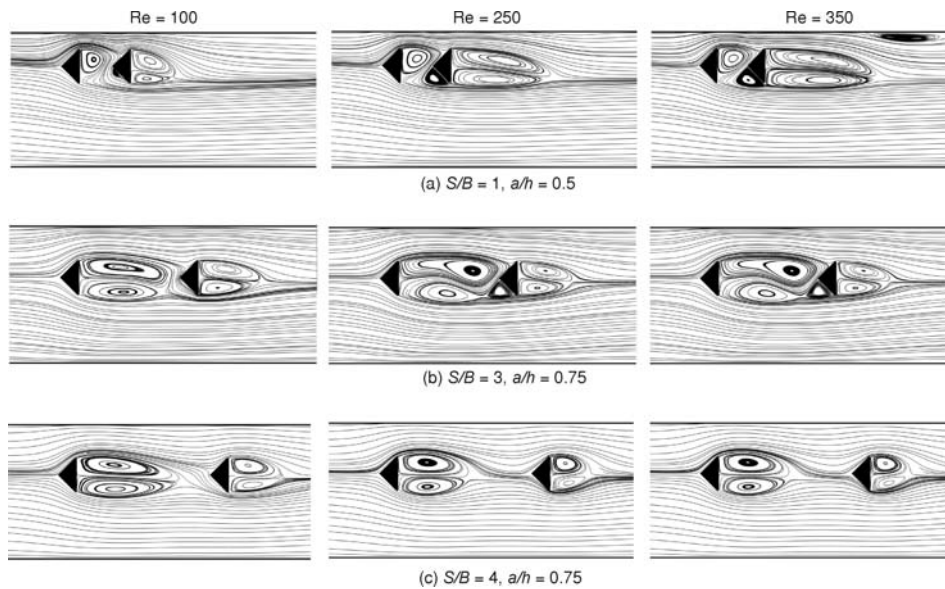
Re = 100   Re = 250   Re = 350

(a) S/B = 1, a/h = 0.5

(b) S/B = 3, a/h = 0.75

(c) S/B = 4, a/h = 0.75

Figure 4. Time-averaged streamlines at different Reynolds number, *S/B*, and *a/h*

By increasing the Reynolds number at *S/B* = 4 and *a/h* = 1, momentum increases thus vortex shedding was removed in the gap distance between two triangle and formed a steady recirculation zone at this area – figs. 5(b). But at *S/B* = 4 and *a/h* = 0.75 for all three Reynolds numbers, vortex shedding can be observed in the gap distance between two squares – figs. 5(b) and 4(c). It should be mentioned that at *a/h* = 0.5 for all *S/B* there is not any vortex shedding at all Reynolds numbers in the gap between two triangles. On the other hand as obstacles approach the wall, at *a/h* = 0.5 for *S/B* = 1, 2, and 3 vortex shedding is removed at all three Reynolds numbers between two triangles and the downstream of the second triangle – figs. 5(a). At *S/B* = 4 , the
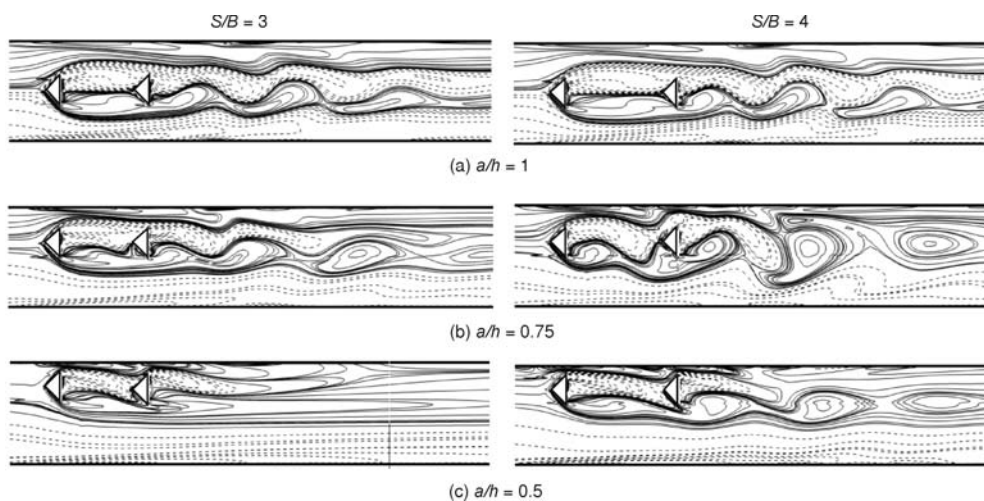

S/B = 3   S/B = 4

(a) a/h = 1

(b) a/h = 0.75

(c) a/h = 0.5

Figure 5. Instantaneous vorticity contours for different wall approach ratios (*a/h*) at Re = 250

190

Mohsenzadeh, A., *et al.*: Convective Cooling of Tandem Heated Triangular Cylinders ...
THERMAL SCIENCE: Year 2010, Vol. 14, No. 1, pp. 183-197

momentum increased at the distance between obstacle and the channel walls so it causes that the wall damping effect on the vortex generation disappears. Therefore vortex shedding is created at Re = 250 and 350 for $S/B = 4$, $a/h = 0.5$ in the downstream of the second triangle – figs. 5(b). With increasing the distance between obstacles and channel's wall at $a/h = 0.75$ and 1, vortex shedding is created at the downstream of the second obstacle for all S/B.

The Strouhal number is investigated to consider the frequency of vortex shedding. Figure 6 shows the variation of the Strouhal number (St) with Reynolds number for different gap spacing S/B and wall approach ratio a/h. It is observed that by approaching the wall, St number decreases and become zero for wall approach ratio equal 0.5. This is true for $S/B = 1$ to 3 at all Reynolds number and only $S/B = 4$ at Re = 100. With increasing space between two triangles, St number increases for $a/h = 1$ while it decreases for $a/h = 0.75$.

One of the main parameter which affected by wall proximity is drag coefficient. Wall proximity has different effect on drag coefficient of the first and second triangles. Figure 7 shows the variation of the drag coefficient with Reynolds number for different wall approach ra-
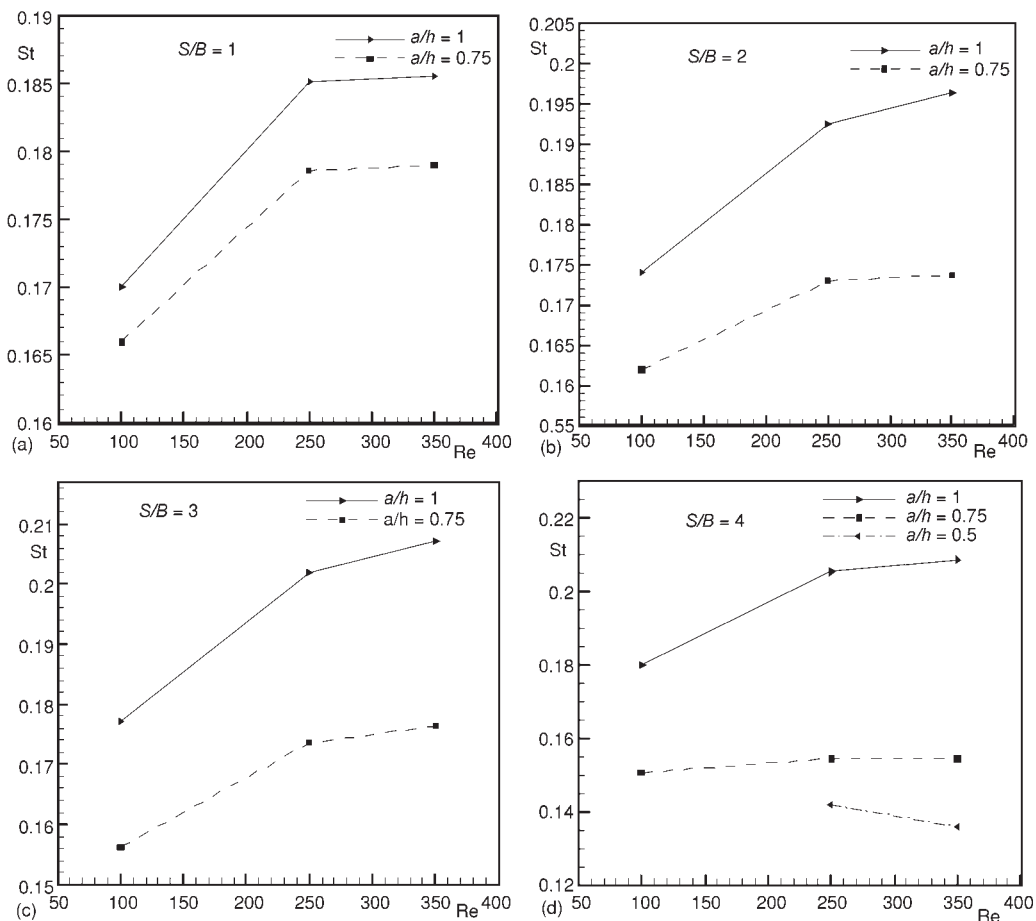

Figure 6. Variation of Strouhal number with Reynolds number for different wall approach ratios *a/h* and *S/B*

tio *a/h* and *S/B*. From *S/B* = 1 to 3 that vortex shedding does not appear in the gap between two triangles, with approaching obstacles to the wall drag coefficient decreases for first triangle but a different behavior is seen for second triangle. This is due to circulation zones that are formed between two obstacles and make a negative drag coefficient for *a/h* = 1 and 0.75. By approaching the wall the vortex formation is changed between two cylinders so increasing the drag coefficient is observed for *a/h* = 0.5 in comparison with other *a/h*. The greatest effect of the gap spacing can be observed at *S/B* = 4. As mentioned before, it is due to the vortex formation in the gap between two triangles which appears at gap spacing.
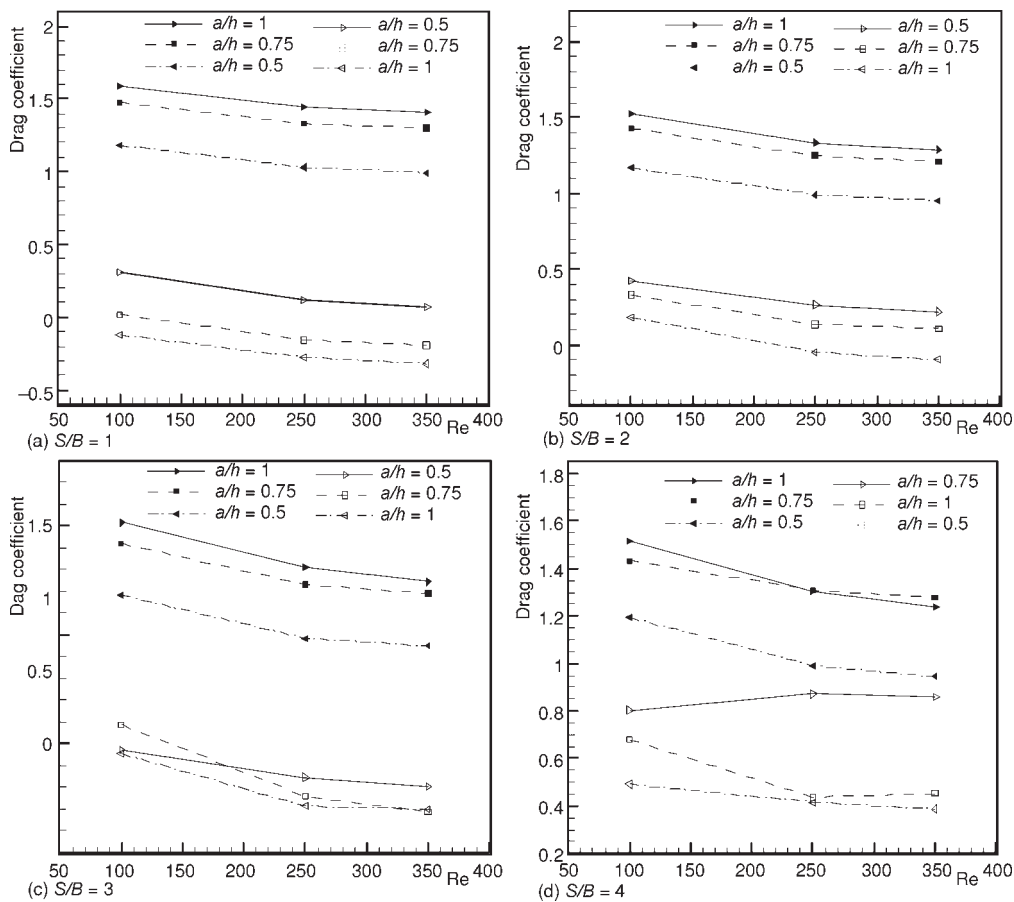

Figure 7. Variation of drag coefficient with Reynolds numbers for different wall approach ratio *a/h* and *S/B* (fill and hollow symbols were used for triangle 1 and 2, respectively)

Heat transfer

In this part the effect of gap spacing, wall approach ratio, and Reynolds number on the convective heat transfer over the triangles is explained. Instantaneous temperature contours are shown in fig. 8. As expected, the flow field has a main effect on convective heat transfer. The locked recirculation region between the triangles causes the increase of temperature in this area
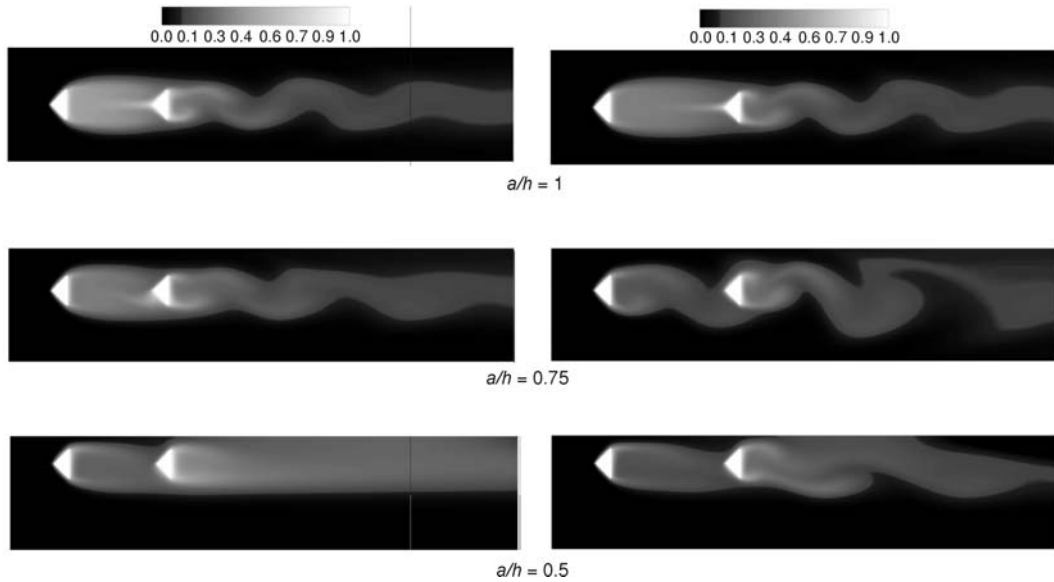
Figure 8. Instantaneous temperature contours for different *a/h* at Re = 250 for *S/B* = 3 (right) and *S/B* = 4 (left)

that decreases the Nusselt number. With approaching the wall, fluid between two obstacle is allowed to pass through them, subsequently increases the heat transfer for upper side of second triangle and rear side of first triangle locally (see fig. 10), but a different behavior was seen in downstream of second triangle as a consequence of suppressing flow influenced by wall (see fig. 8).
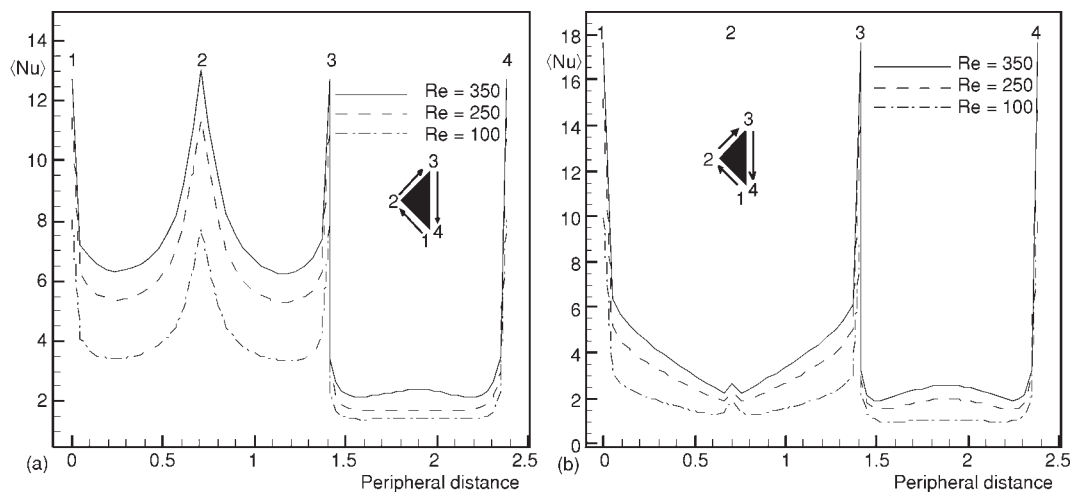

Figure 9. Time-averaged local Nusselt number distribution over the triangle surfaces for different Reynolds numbers at *S/B* = 3 and *a/h* = 1; *(a) first triangle, (b) second triangle*
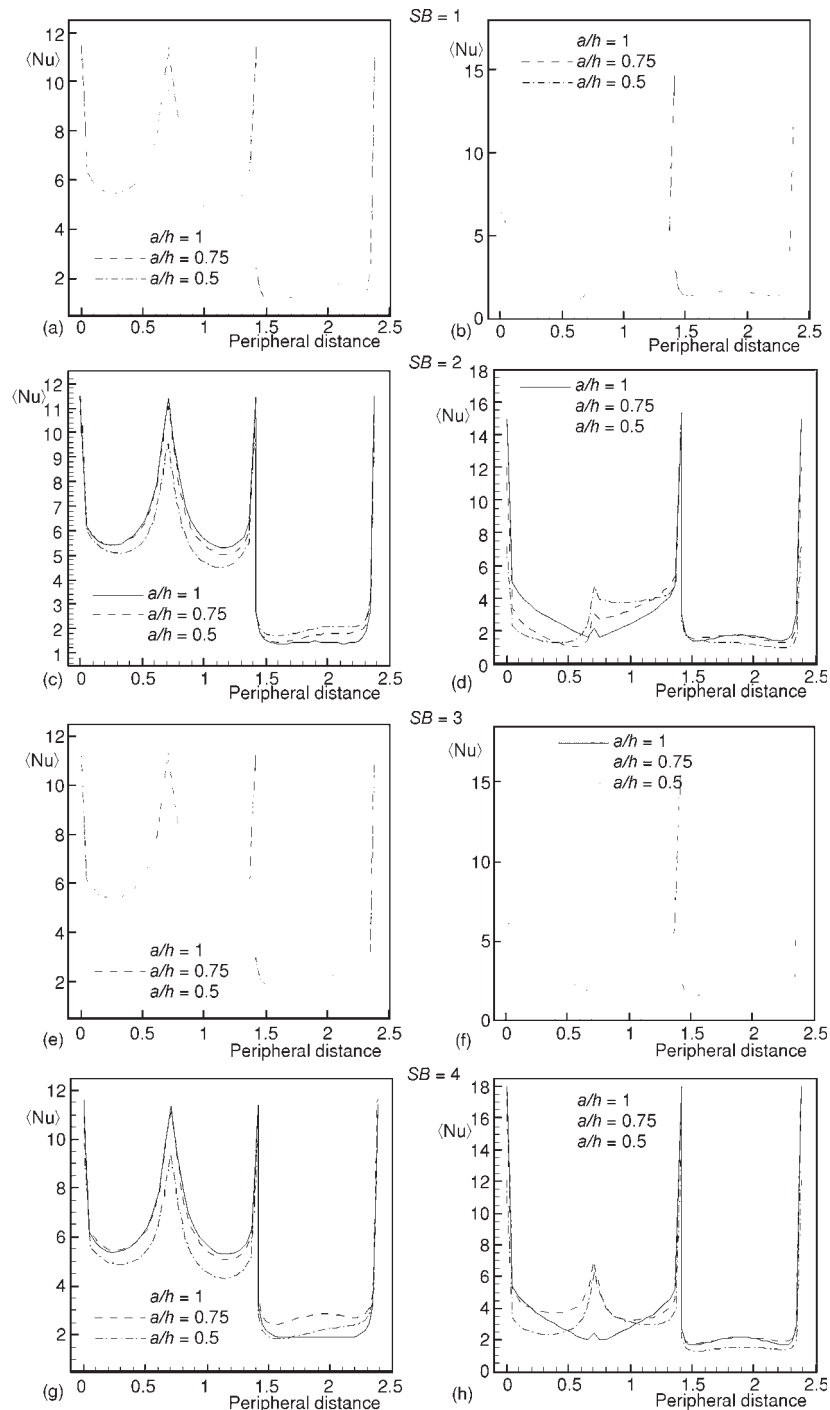
Figure 10. Time-averaged local Nusselt number distribution over the triangle surfaces for different *S/B* and *a/h* at Re = 250; first triangle (left) and second triangle (right)

194

Mohsenzadeh, A., *et al*.: Convective Cooling of Tandem Heated Triangular Cylinders ...
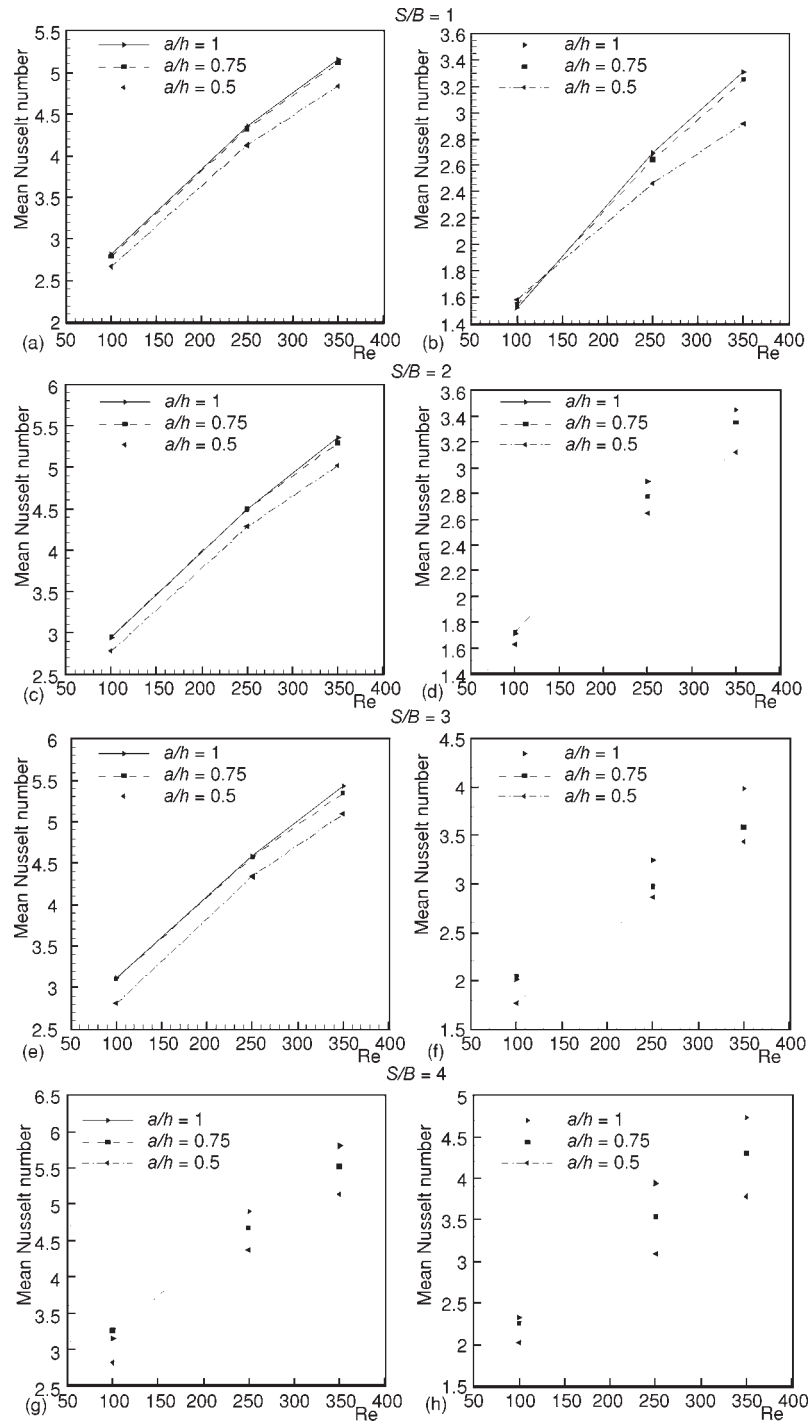THERMAL SCIENCE: Year 2010, Vol. 14, No. 1, pp. 183-197

Figure 11. Variation of total time-averaged Nusselt number *vs*. Reynolds number at different *S/B* and *a/h*; first triangle; (left) and second triangle (right)

The time-averaged local Nusselt number distribution over the triangle surfaces was plotted in figs. 9 and 10. In fig. 10, the time-averaged local Nusselt number distribution over the first and second triangle surfaces at $S/B = 3$, $a/h = 1$ for different Reynolds number have been compared. A different behavior is seen for first and second triangle .Velocity boundary layer begin at the apex of triangle for first triangle so local Nusselt number in this point is greater than other point in around it but for second triangle boundary layer end in the apex of triangle.

In fig. 10 the effect of wall approach ratio at Re = 250, on the local Nusselt number for different S/B has been shown. As obstacles approach to the wall, local Nusselt number at upper side become greater than lower side for the first triangle. It is due to the less momentum passes along the upper side than lower side but for second triangle a circulation zone that was formed along the lower side decreases Nusselt number. This circulation zone is less serious for upper side, so unlike the first triangle, Nusselt numbers for upper side become greater than lower side of second triangle. With approaching the wall two main parameters affect the variation of Nusselt number. As obstacles approach the wall, strength of momentum force decreases and it causes Nusselt number to decrease on the other hand with approaching the wall, the circulation zone that is formed in the gap between two obstacles did not fill the gap between two obstacles completely and as mentioned before, flow between two triangles can stream out of that area, especially in the low Reynolds number. This phenomenon causes Nusselt number to increase. For first triangle first parameter is more important so from $S/B = 1$ to $S/B = 3$ Nusselt number at $a/h = 0.5$ is smallest although Nusselt number is fairly same for $a/h = 1$ and 0.75 specially at lower Reynolds number (Re = 100, 250). For second triangle the second parameter becomes more serious specially at low Reynolds number. These two reversed parameter causes that Nusselt number at second triangle for $S/B = 1$ becomes greater for $a/h = 0.5$ than $a/h = 0.75$, and 1 at Re = 100 and also become greater for $a/h = 0.75$ than $a/h = 1$ at Re = 100 in the $S/B = 2$ and 3 (see fig. 11). The vortex formation in the gap distance has a main effect on the heat transfer over the triangles. It should be mentioned that from $S/B = 1$ to $S/B = 3$ there is not any vortex shedding in the region between two obstacles but at $S/B = 4$, $a/h = 0.75$. By increasing the gap spacing between triangles, vortex sheds in this region at all three Reynolds numbers. This caused that the Nusselt number become greater for $a/h = 0.75$ than $a/h = 1$ even at higher Reynolds number for both first and second triangles (see fig. 11 for Re = 250 and 350).

Conclusions

The effect of wall proximity of two isothermal tandem triangle cylinders on fluid flow and heat transfer for different gap spacing is investigated numerically in a horizontal plane channel. The main results are summarized as follows.

From S/B 1 to 3, vortex dos not shed in the gap between two obstacles at any a/h. Same behavior is observed with increasing S/B in fluid characteristic and heat transfer.

For $S/B = 1$ to 3 with approaching the wall, vortex shedding disappears in downstream of second triangle at $a/h = 0.5$, and St numbers decreases and be zero for wall proximity equal 0.5 at all Reynolds numbers. Drag coefficient decreases for first triangle while for second triangle, a complete different behavior is observed except at $S/B = 3$, $a/h = 0.75$, and 1 for Re = 100.

The greatest effect of the gap spacing can be observed at $S/B = 4$. In this case, vortex shedding created at gap spacing between two triangles for Re=100 at $a/h =1$ and also for all three Reynolds numbers at $a/h = 0.75$. On the other hand, vortex shedding can be observed in the down stream of second triangle at $a/h = 0.5$ for Re = 250 and 350. These caused that drag coeffi-

Mohsenzadeh, A., *et al.*: Convective Cooling of Tandem Heated Triangular Cylinders ...

196   THERMAL SCIENCE: Year 2010, Vol. 14, No. 1, pp. 183-197

cient for *a/h* = 0.75 become greater than *a/h* = 0.5, and 1 for second triangle. This phenomenon effects on the heat transfer from the second triangle.

Nomenclature

A – surface area of the bluff body, $[m^2]$
a – distance of the apex of triangles from the upper wall of channel, $[-]$
a/h – wall approach ratio, $[-]$
B – triangle width, $[m]$
C_d – drag coefficient $[FD/(0.5\rho u_{max.}^2 A)]$, $[-]$
FD – drag force, $[N]$
f – eddy-shedding frequency, $[-]$
H – channel width, $[m]$
h – half of the channel width, $[m]$
$\underline{Nu}$ – local Nusselt number, $[-]$
$\overline{Nu}$ – streamiwse averaged Nusselt number, $[-]$
$\langle Nu \rangle$ – time-averaged Nusselt number, $[-]$
p – dimensionless pressure, $(p^*/\rho u_{max.}^2)$, $[-]$
p^* – pressure, $[Nm^{-2}]$
Pr – Prandtl number ($= \nu/\alpha$), $[-]$
Re – Reynolds number ($= u_{max.}B/\nu$), $[-]$
S/B – gap between two triangle, $[-]$

St – Strouhal number ($= fB/u_{max.}$), $[-]$
T – temperature, $[K]$
t – time, $[s]$
U – mean dimensinless velocity, $[-]$
u, v – dimensionless velocity($(u^*,v^*)/u_{max.}$), $[-]$
u^*,v^* – velocity components, $[ms^{-1}]$
x, y – dimensionless coordinates, $[-]$
x^*,y^* – Cartesian coordinates, $[m]$

Greek symbols

τ – dimensionless time, $[-]$
θ – dimensionless temperature, $[-]$
ν – kinematic viscosity, $[m^2 s^{-1}]$

Subscripts

C – cold
H – hot

Reference

[1] Alonso, G., Meseguer, J., A Parametric Study of the Galloping Stability of Two-Dimensional Triangular Cross-Section Bodies, *J. Wind Eng. Ind. Aerodyn, 94* (2006), 4, pp. 241-253

[2] Buresti, G., Lombardi, G., Talamelli, A., Low Aspect-Ratio Triangular Prisms in Cross-Flow: Measurements of The Wake Fluctuating Velocity Field, *J. Wind Eng. Ind. Aerodyn., 74-76* (1998), April, pp. 463-473

[3] Csiba, A. L., Martinuzzi, R. J., Investigation of Bluff Body Asymmetry on The Properties of Vortex Shedding, *J. Wind Eng. Ind. Aerodyn.*, *96* (2008), 6-7, pp. 1152-1163

[4] Ulrichs, E., Herwig, H., Between Two Limits: Flow Separation Behind a Bluff body Close to a Wall, *Forschung im Ingenieurwesen, 68* (2003), 1, pp. 36-38

[5] Camarri, S., Salvetti, M. V., Buresti, G., Large-Eddy Simulation of the Flow Around a Triangular Prism with Moderate Aspect Ratio, *J. Wind Eng. Ind. Aerodyn, 94* (2006), 5, pp. 309-322

[6] Abbassi, H., Turki, S., Ben Nasrallah, S., Numerical Investigation of Forced Convection in a Horizontal Channel with a Built-in Triangular Prism, *Int. J. Thermal Science, 40* (2001), 7, pp. 649-658

[7] Chattopadhyay, H., Augmentation of Heat Transfer in a Channel Using a Triangular Prism, *Int. J. Thermal Sciences, 46* (2007), 5, pp. 501-505

[8] Martinuzzi, R. J., Bailey, S. C. C., Kopp, G. A., Influence of Wall Proximity on Vortex Shedding from a Square Cylinder, *Experiments in Fluids, 34* (2003), 5, pp. 585-596

[9] Bailey, S. C. C., Martinuzzi, R. J., Kopp, G. A., The Effects of Wall Proximity on Vortex Shedding from a Square Cylinder: Three Dimensional Effects, *Physic of Fluids, 14* (2002), 12, pp. 4160-177

[10] Bosch, G., Kappler, M., Rodi, V., Experiments on the Flow Past a Square Cylinder Placed Near a Wall, *Exp. Thermal Fluid Science, 13* (1996), 3, pp. 292-305

[11] Chakrabarty, D., Brahma, R., Effect of Wall Proximity in Fluid Flow and Heat Transfer from a Square Prism Placed Inside a Wind Tunnel, *Thermal Science, 11* (2007), 4, pp. 65-78

[12] Singha, A. K., Sarkar, A., De, P. K., Numerical Study on Heat Transfer and Fluid Flow Past a Circular Cylinder in the Vicinity of a Plane Wall, *Numerical Heat Transfer, PartA, 53* (2008), 6, pp. 641-666

[13] Rosales, J. L, Ortega, A., Humphrey, J. A. C., A Numerical Simulation of the Convective Heat Transfer in Confined Channel Flow Past Square Cylinders: Comparison of Inline and Offset Tandem Pairs, *Int. J. Heat Mass Transfer, 44* (2001), 3, pp. 587-603

[14] Valencia, A., Numerical Study of Self-Sustained Oscillatory Flows and Heat Transfer in Channels with a Tandem of Transverse Vortex Generators, *Heat and Mass,Transfer, 33* (1998), 5, pp. 465-470

[15] Farhadi, M.,Sedighi, K., Madani, M. M., Convective Cooling of Tandem Heated Squares in a Channel, *Proc. IMechE Part C: J. Mechanical Engineering Science*, *223* (2009), 4, pp. 965-978

[16] Farhadi, M., Sedighi, K., Madani, M. M., Convective Cooling of Tandem Heated Squares in a Channel. *Proceedings*, 3rd BSME-ASME International Conference on Thermal Engineering, 2006, Dhaka, Bangladesh

[17] Etminan, E., Sohankar, A., Numerical Simulation of Flow around of Two Tandem Squares, *Proceedings*, 10th Annual Conference of Fluid Dynamic, Yazd, Iran, 2006

[18] Sumner, D., Richards, M. D., Akosile, O. O., Two Staggered Circular Cylinders of Equal Diameter in Cross-Flow, *Fluids and Structures, 20* (2005), 2, pp. 255-276

[19] Zdravkovich, M. M., Flow Around Circular Cylinders, Vol. 1: Fundamentals, Oxford University Press, Oxford, UK, 1997

[20] Kostic, Z., Oka, S., Fluid Flow and Heat Transfer with Two Cylinders in Cross Flow, *Int. J. Heat and Mass Transfer, 15* (1972), 2, pp. 279-299

[21] Akbari1, M. H., Price, S. J., Numerical Investigation of Flow Patterns for Staggered Cylinder Pairs in Cross-Flow, *Fluids and Structures, 20* (2005), 4, pp. 533-554

[22] Buyruk, E., Numerical Study of Heat Transfer Characteristic on Tandem Cylinder, Inline and Staggered Tube Bank in Cross Flow of Aair, *Int. Comm. Heat Mass Transfer, 29* (2002), 3, pp. 355-366

[23] Nourollahi, M., Generation of CFD Code for Solving the Fluid Governing Equations in Non-Orthogonal Coordinate Systems, M. Sc. thesis, Faculty of Mechanical Engineering, Babol Noshirvani University of Technology, Babol, Iran, 2007

[24] Ferziger, J. H., Peric, M., Computational Methods for Fluid Dynamics. Springer-Verlag, Berlin Heidelberg, New York, 2002